THE AMERICAN SOCIETY OF MECHANICAL ENGINEERS
345 E. 47th St., New York, N.Y. 10017

96-GT-514

DATA TRANSMISSION SYSTEMS FOR A TRANSIENT GAS TURBINE ROOTOR

Catherine M. Byrne and Mark R. D. Davies
Department of Mechanical and Aeronautical Engineering
University of Limerick
Limerick
Ireland

ABSTRACT

The design and testing of multi-channel data transmission systems for a transient turbine test rotor are presented. Two multi-channel systems were required for the conditioning and transmission of the electrical signals from thin film gauges and un-packaged embedded pressure transducers which are to be used for the measurement of rotor blade surface heat transfer and pressure respectively. All measurements will be taken from the same rotor at design Mach and Reyoolds numbers. Signal conditioning and amplification will be performed in the rotating frame to solve the problems associated with accurate sigoal transmission. Also, the use of a multi-chanoel array of light emitting diodes for data transmission is described which allows accurate signal reconstruction. Both systems have been initially stress screened and are shown to have an adequate bandwidth for resolving wake blade interactions.

NOMENCLATURE

C	Electrical Capacitance
F(s)	Loop filter transfer fuoction
F_o	V/F output frequency
G_{u4}	Gain of U4 (fig. 5)
G_{fc}	Circuit gain
$H(\omega)$	Circuit transfer function
R	Electrical resistance
T	Temperature
V	Voltage
V_G	Heat transfer gauge voltage
V_{gi}	Initial heat transfer gauge voltage (t=0)
V_d	Phase detector output voltage
V_{os_1}	Stage 1 Voltage output
V_{os_2}	Stage 2 output voltage
V_{os_3}	Stage 3 output voltage
V_f	Loop filter output voltage
Z_i	Input circuit impedance
Z_o	Output circuit impedance
Z_f	Feedback circuit impedance
q	Heat flux rate

Greek		*Subscripts*	
ω	Frequency	in	input
ω_n	Natural frequency	out	output
ϕ	Phase	ref	reference
$\Delta\phi$	Phase difference	s	surface
ξ	Damping factor	6	U4 pin 6 (fig. 5)

INTRODUCTION

All turbine research is aimed at improving the cost effectiveness of the design process, the efficiency of the ensuing desigo and lengthening of the time between maintenance checks for the operational turbine. To achieve this, fast accurate and reliable computational predictions are required. It is widely accepted that the currently available computational codes canoot be relied upon to predict the positioa of turbine blade boundary layer transition or the subsequent turbulent flow, Denton (1993). Many problems associated with this failure stem from the unsteady interactions between the

Presented at the International Gas Turbine and Aeroengine Congress & Exhibition
Birmingham, UK — June 10-13, 1996

rotating and stationary blade rows, Doorly (1985a, 1985b, 1989), and Dunn et al. (1984, 1986). The region of transition moves as the vane wakes and shocks pass through the rotor and the scale of the boundary layer turbulence is partly dependant upon the free stream unsteadiness, Dring (1982) and Hodson (1983). Thus, there is a continuing need for experimental data from rotating facilities.

Although considerable turbine rotor blade research has been undertaken in the past, Dunker (1995) indicated the need to establish a database on the flow structure and heat transfer around uncooled rotor blades behind a transonic stator with trailing edge cooling. Purely aerodynamic phenomena are usually investigated in cold flow continuous turbines. For the measurement of blade surface heat transfer rates and temperatures, transient flow turbines are used. Although it has been shown that these may be used equally well for aerodynamic measurements, The European Union has recently funded the development of two rotating turbine test facilities at DLR, Goettingen and The von Karman Institute (VKI). The first is a modification of the DLR cold flow facility and the second a modification of the VKI annular cascade piston tube tunnel. The turbines are to run with the same profile at the same Mach and Reynolds numbers with DLR concentrating on laser and surface mounted hot film transition gauges and VKI on rotating pressure and heat transfer measurements. There will also be a number of measurements to prove the similarity of the rotors. This paper describes the development of rotating instrumentation modules for the VKI turbine stage, which has been designed to use the existing piston tube, Sieverding and Arts (1992), with a rotor placed downstream from the annular guide vane cascade, in a similar manner to that adopted at Oxford, Ainsworth et al. (1988b)

The primary design requirement for such instrumentation modules is that the signal be transmitted from the rotor with the highest fidelity. To achieve this, the signals must be amplified to raise them above the level of the transmission noise. Thus, a significant amount of the signal conditioning needs to be performed in the rotating frame. The space available for this is found inside the turbine shaft and the systems must therefore be compact and robust enough to withstand the rotating stresses.

Two multichannel instrumentation systems are described in this paper : the first is for 24 thin film blade mounted heat transfer gauges and the second for 24 blade mounted pressure transducers. Each system is mounted on circuit boards in the turbine shaft and each is connected to the same transmission system that delivers the data from the rotating frame via light emitting diodes as opposed to the previous method of using slip rings. It is important to note that by using these infra-red emitting diodes, the noise level is low and there is no wear. For silver contact slip-rings, typical life times stated are less than 1000 hours and this is far less than expected from the optical system. In comparsion with commerical optical systems, most available are single channel, end of shaft mounted. No sensible speed limitation on the design concept can be seen so it can be applied to high speed turbine applications. A high speed contact system, with contact resistance, also needs to be air cooled.

The development of these systems and their testing prior to installation on the turbine rotor is described. The overall design approach is to design separate systems for the heat transfer gauges and pressure transducers which will be installed as required. The paper first describes the heat transfer and pressure transducer electronics then the transmission system followed by the laynut and operation of the complete system.

HEAT TRANSFER CIRCUITRY

To design an efficient turbine cooling system, it is necessary to know the distribution of the uncooled blade Nusselt number. In the VKI turbine stage, this will be measured by painted thin film gauges on macor or machinable glass ceramic substrates inserted into the turbine blade. The idea of painting thin film gauges on macor was originally pioneered by Oxford University, Oldfield et al. (1978). These inserts will be deep enough for a nne dimensional semi-infinite theory to be used to convert the surface temperature into a surface heat transfer rate. The turbine flow duration is of order 0.5 seconds and the stage is scaled on Reynolds and Mach numbers, blade to gas temperature ratio and rotational geometry, Davies and Wallace (1995). Mid-span mounted gauges will give the chord wise variation of Nusselt number and as the frequency response is high, will allow the nature of the blade vane interaction to be described. Factors of cost, space and data requirements led to the following specification being agreed upon between the authors and the von Karman Institute.

Heat Transfer Circuit Specification

- 24 heat transfer gauges will be used for surface temperature measurements and will be divided into two groups of 12 with one group operating at any one time. All gauges are to mounted on the mid-span of the rotor blade.
- As 12 gauges are operating at any one time, 12 transmissinn channels are required to transmit the signals from the rotating to the stationary frame.
- The surface temperature signals will be converted from a voltage to a frequency signal before transmission and then transmitted optically.
- With a rotational speed of 6500 rpm, the blade passing frequency is expected to be 4600 Hz
- Switching between these groups will be performed electronically and will take place between tunnel runs
- The maximum gauge voltage is estimated at 0.75V with a 10mA constant current supply.
- Gauge signal amplification will increase with increasing frequency to compensate for the gauge response.
- The circuitry is required to have a bandwidth of 25KHz.
- An auto-zeroing circuit will zero the output voltage before each run.
- All boards will be stress screened by spin testing to a speed of 6,000 rpm.

- The circuit boards will connect to a permanently positioned transmission system inside the rotor hub.
- The inside dimensions of the turbine shaft available for the instrumentation system are 540mm length by 70mm diameter allowing room for two permanently fixed transmission boards and two heat transfer boards placed side by side.

Heat Transfer Electronic Design

A block diagram of the heat transfer circuitry is given in Fig. 1.

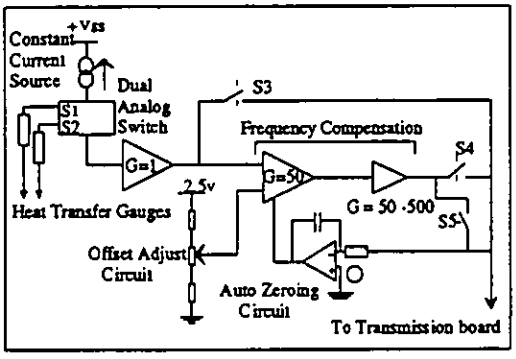

Fig.1. Single Channel Heat Transfer Block Diagram

Each gauge is energised by a precision constant current source of 10mA, +/-1%, giving a voltage which is linearly proportional to the surface temperature signal, this voltage is then amplified to enable accurate signal transmission. The gain is designed to vary over the frequency range from 0 to 25KHz. An autozeroing circuit is used on all channels to ensure that the circuit output voltage before a run is zero. Analog switches are used to switch between the two groups of twelve gauges and also to switch between a gain of 1, to measure the gauge voltage before a run, and the frequency variable gain of 50-500.The necessity for the variation of gain with frequency is discussed by Ainsworth et al. (1988a) when using a two layered substrate to mount gauges for transient heat transfer measurements. The sensitivity of the heat transfer gauges falls as a square root of frequency, in line with the semi-infinite theory.

Therefore, the ratio of surface flux to surface temperature changes as a function of frequency and because of this, the signal-to-noise ratio can decrease with increasing frequency. Since there is particular interest in the high frequency information, the signal to noise ratio is improved by amplifying the higher frequency information before transmission. For the purpose of this experiment, the gauges are painted directly onto ceramic which is thick enough to be considered as a semi-infinite substrate for the time scale of the test. As a result, the ratio of the flux to surface temperature is found to be proportional to the square root of frequency over the entire frequency range, causing a decrease in the signal to noise ratio. Below approximately 35Hz, the attenuation of the temperature signal with frequency is not expected to be significant and therefore, the circuit has been designed to further amplify the signal in the range 35Hz to 25KHz.

The requirement for frequency compensation in this design is that the system should have a constant gain of 50 up to 35 Hz, a gain increase of 50 to 500 between 35 Hz and 3500 Hz in line with the semi-infinite theory, and a constant gain of 500 between 3.5 and 25 KHz after which the gain will start to decrease. To achieve this, the compensation network is divided into three secuions : with reference to Fig. 3, the first section is designed around an AD524 low noise, low non linearity and low offset voltage drift instrumentation amplifier (U4), designed to have a gain of 50 with a required bandwidth of 25 KHz. This amplifier has two input signals, the first is the gauge voltage and the second is a reference voltage created by a potential divider circuit with a range of 0.5V to 1.267V. This voltage will be set before the boards are installed into the rotor and will correspond to a known gauge voltage. The second and third stages make up the gain shaping part of the complete circuit and a block diagram of the stage 2 and 3 gain is given in Fig. 2.

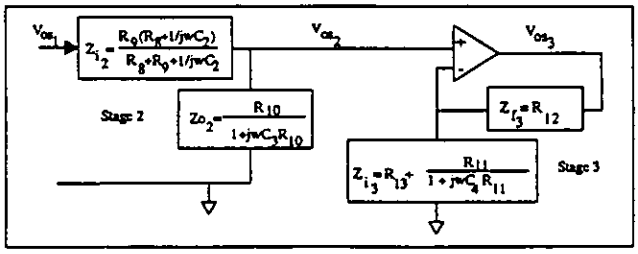

Fig. 2. Block diagram of frequency compensation circuit. (See Fig. 3 for definition of terms)

Stage 2 forms a lead-lag network showing characteristics of both lead and lag circuits and this stage contains breakpoints at 66 Hz, 200 Hz and 27.77 KHz respectively. The third stage forms a lead network and the amplifier of this stage, U7 in Fig. 3, may be modelled as a simple feedback circuit as shown in Fig. 2 configured in non-inverting mode with a gain of $1+Z_{f_3}/Z_{i_3}$. The gain of the amplifier is designed to vary with frequency using a variable impedance in the feedback leg. Analysis of this model leads to the calculation of breakpoints at 566 Hz and 1.759 KHz. The combined gain of stage 2 and 3 is described by Eq. 1, where Z_{i_2}, Z_{o_2}, Z_{i_3} and Z_{f_3} are defined in Fig. 2.

$$\frac{V_{os_2}}{V_{os_1}} = \frac{Z_{o_2}(Z_{i_3}+Z_{f_3})}{Z_{i_3}(Z_{o_2}+Z_{i_2})} \qquad (1)$$

Rewriting Eq. 1 in terms of the component values in Fig. 3 the gain as a function of frequency is:

$$\frac{V_{os_2}}{V_{os_1}} = \frac{R_{10}\left[1+j\omega C_2(R_8+R_9)\right]\left[R_{12}+R_{11}+R_{13}+j\omega C_4 R_{11}(R_{12}+R_{12})\right]}{\left[R_{10}\left[1+j\omega C_2(R_8+R_9)\right]+R_9\left[1+j\omega C_3 R_{10}\left[1+j\omega C_2 R_8\right]\right]\right]\left[(R_{11}+R_{13})+j\omega C_4 R_{11}R_{13}\right]} \qquad (2)$$

The overall gain of the system is defined as being:

$$G_{fc} = \frac{V_{os_3}}{(V_G - V_{ref})} = G_{b4}\frac{V_{os_3}}{V_{os_1}} \quad (3)$$

where $G_{U4} = 1 + \frac{40,000}{R_3 + R_4}$ (4)

Frequency and phase response curves showing predicted and measured values are given in Fig. 4. Due to the nature nf the design and the choice of components, the system has a gain of 57 at 35Hz, 474 at 3.5 KHz and 362 at 25KHz.

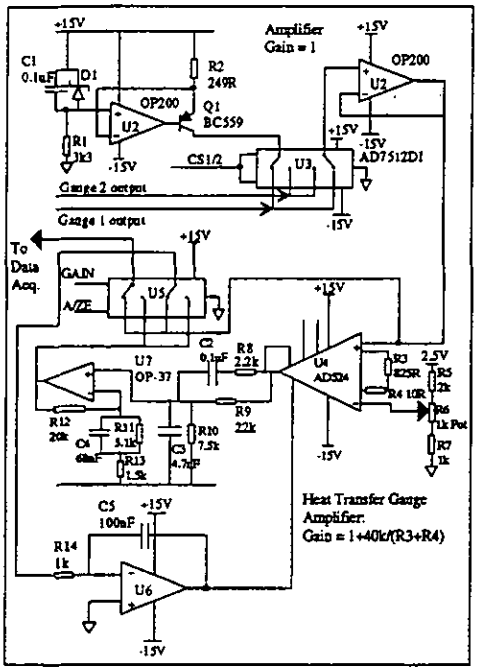

Fig. 3. Single Channel Heat Transfer Gauge Circuit Diagram

To assist in the design of the frequency compensation networks, a version of a SPICE (*Simulation Program with Integrated Circuit Emphasis*) package called PSPICE was used to simulate the operation of the two separate circuits used to make up the complete network. The circuit can be inputted in the form of either a circuit schematic diagram or a netlist describing which components are connected to which through a series of nodes. The latter method was chosen for the purpose of the preceding design. The netlist must also include the amplitude level and the range of frequencies of the input signal to the simulated circuit. Figure 4 shows the accuracy of the prediction in comparison to the measured frequency response.

Just before a turbine test run, any difference which exists between the reference and the gauge voltage signals, which form the two inputs to U4 in Fig. 3, needs to be eliminated so that the circuit exhibits zero output voltage. This is achieved using an autozeroing circuit which is based around an AD711 operational amplifier, U6, configured as a sample-and-hold amplifier. All channels require 2 CMOS analog switch I.C's, AD7512 with each I.C containing two

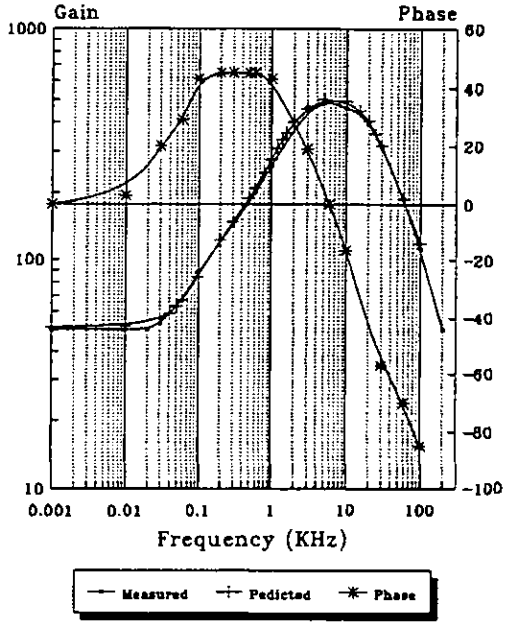

Fig. 4. Frequency Response and Phase curve of compensation circuit

Single Pole Double Throw (SPDT) switches with a low on resistance of 75R and a low leakage current of 500pA. One I.C allows switching between each pair of gauges and the other allows the autozeroing circuit to be switched in at the appropriate time and also allows switching between a gain of 1 and a variable gain of between 50 and 500. Two strobing signals are required to control the switching on all channels plus nne to perform autozeroing and these signals will be generated from the stationary frame and transmitted to the signal conditioning circuitry via slip-rings. With reference to Fig. 3, these strobing signals are labelled A/ZC for autozeroing. CS1/2 for gauge selection and GAIN to select the required gain. Figure 5 illustrates the timing diagram for the sequence of events. Initially, setting the GAIN strobe signal high will allow the gauge voltage before a run to be measured. Autozeroing will be performed by maintaining the GAIN strobe signal high and changing the autozeroing (A/ZE) strobe line from low to high before a run and this will eliminate any difference that exists between the gauge voltage and the reference voltage on the input to the instrumentation amplifier. After autozeroing the voltage appearing on pin 6 of the instrumentation amplifier, U4, is :

$$V_6 = -\frac{G_{U4}R_{10}(V_{gi} - V_{ref})[(R_{12} + R_{11} + R_{13})]}{[R_{10} + R_9][(R_{11} + R_{13})]} \quad (5)$$

Immediately before a run, the autozeroing strobe line will be switched from high to low. As the gauge voltage varies the output of the circuit is calculated as :

$$V_o = G_{fc}(V_G - V_{ref}) + V_6 \qquad (6)$$

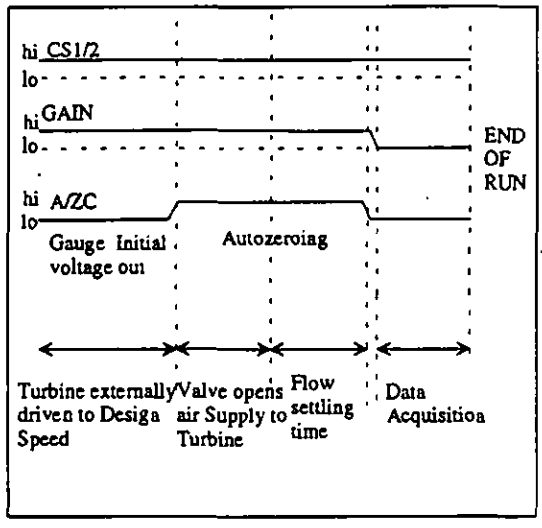

Fig.5. Heat Transfer Circuit Timing Diagram

PRESSURE TRANSDUCER CIRCUIT DESIGN

Pressure transducers, described by Ainsworth et al. (1991), will be used to measure the steady and unsteady mid-span pressure distribution. As with the heat transfer gauges, these will connect to the transmission system fitted into the rotor hub. For pressure transducers thermal sensitivity is one of the biggest sources of error and temperature changes can affect the transducers' offset and pressure sensitivity. If these two seasitivities are known and the temperature of the bridge is measured in conjunction with the output, the transducer output may be corrected for temperature effects. This implies that in addition to pressure, a signal proportional to the mean gauge temperature must be transmitted.

Specification

- 24 pressure transducers without packaging will be laid onto the surface of three blades with 8 transducers per blade.
- Only one instrumeated blade will be installed per run to reduce the likelihood of gauge stress failure.
- Each transducer will be powered by a separate high stability 10 volt reference voltage.
- Each transducer will have two outputs, one pressure and one temperature sigaal which will require a transmission channel each giving a total of 16 transmission channels required.
- Both the pressure and temperature signals will require amplificatioa before transmission and the amplification will be of the order 25 for both.
- No electronic switching will take place between channels.
- The system will be stress screened by spin testing at 6000rpm.
- The pressure transducer amplifier is required to have a bandwidth of 100KHz and the sense resistor amplifier bandwidth requirement is 400Hz.

Circuit Design

Each transducer consists of a silicon diaphragm with a wheatstone resistor bridge diffused into it's upper surface. The transducer measures pressure induced strain on the bridge. The bridge resistance is in the range 400-1000 ohms. Each transducer requires 4 wires routed down the disc to the transducer amplifier circuit board connector and is powered by a constant high stability 10V reference voltage across the bridge so that the bridge output depends on the balance of the resistors in the bridge. Figure 6 shows a block diagram of the pressure transducer system.

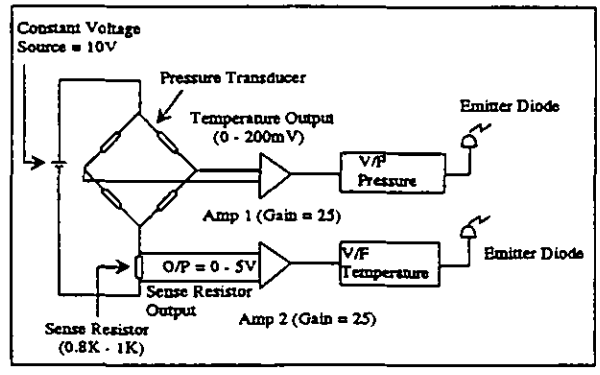

Fig. 6. Pressure Transducer Block Diagram.

When pressure is applied to the transducer, the diaphragm deflects straining these resistors. The resistors are positioned such that two are in tension and two are in compression and therefore to amplify the change in bridge resistance. The pressure transducer signal conditioning circuitry for one channel is shown in Fig. 7. At the heart of the system are two precision instrumentation amplifiers, U2 and U4. U4 has a gain of 25 and converts the pressure transducer bridge output, with a specified voltage range of 0-200mV, from a differential to a single ended signal with a maximum voltage of 5V. Each transducer has a sense resistor located on a separate daughter board which plugs into the main instrumentation board and which is identical in value to the bridge resistance at a known calibration temperature. The pressure transducer mean temperature is measured by sensing the bridge current, which is determined by sensing the voltage across a sense resistor with a low thermal coefficient of resistance connected in series with the bridge. At the calibration temperature, the voltage drop across the sense resistor should be exactly 5 Volts. The signal produced by the sense amplifier (U2) is the deviatinn, which is of the order 0-60mV, from this voltage caused by a change in transducer temperature, this change being amplified by

a factor of 25. Knowing the deviation voltage enables the transducer temperature to be inferred from calibration data previously recorded. As the mean temperature is only required, the signal is filtered with a 2nd order low pass filter (U3) with a 3dB cutoff frequency at 400 Hz as shown in Fig. 8.

No electronic switching is needed between the transducers because the instrumented blades are changed between runs. The frequency response of the sense resistor amplifier and the pressure transducer bridge amplifier was measured on all channels. Typical bode plots for both are shown in Fig. 8 which shows the frequency response curve for the filtered pressure transducer sense amplifier, U2, and this amplifier has a bandwidth of 400 Hz at the -3dB point. Similarly, the pressure transducer bridge amplifier, U4, has an unfiltered bandwidth of 432 KHz at the -3dB point. There is no adjustment facility on the pressure transducer instrumentation boards, but instead, calibration is achieved by adjustment of the receiver boards, which is described in the proceeding section.

TRANSMISSION SYSTEM

A suitable means of transmitting the signals from the rotating frame had to be found with the minimum transmission noise. Ainsworth et al. (1988a) and Dunn et al. (1984) transmitted data using slip-rings but an inherent problem with these systems was the level of the signal-to-noise ratio. Expensive slip-rings are required to keep the signal-to-noise ratio as high as possible. Kappler et al. (1987) developed a method of transmitting the data optically as a series of pulses which improved this ratio and this idea was later improved upon by Sieverding et al. (1992) increasing the bandwidth to 100Khz for a four channel pressure transducer instrumentation system. This design has been improved very slightly to facilitate simultaneous data transmission through 16 channels and a procedure has been developed to allow accurate calibration of each channel to ensure minimum distortion during transmission. The approach is to condition the data in the rotating frame by converting it from a voltage to a frequency signal and then to transmit this signal from the shaft using Light Emitting Diodes (LED's). The signal is then picked up by a light sensitive detector and reconverted to analog form using a Phase Locked Loop (PLL). From the PLL, the signal is transmitted to the data acquisition system. The heat transfer and pressure transducer circuits are designed to utilise the same transmission system. The boards are designed so that they plug directly into the same in-shaft transmission board. Therefore, once the in-shaft transmission boards are installed into the rotor they do not need to be removed until all the heat transfer and pressure data has been gathered. Power to the transmission boards is supplied from the stationary to rotating frame via slip-rings carrying +/- 18V and ground supplies. This supply is broken down to +/-15V using low drop out voltage regulators present on both boards. The transmission boards are used to supply power to the heat transfer and pressure transducer boards, whichever are connected in. The control signals for the heat transfer boards are supplied via slip-rings and routed through the transmission boards.

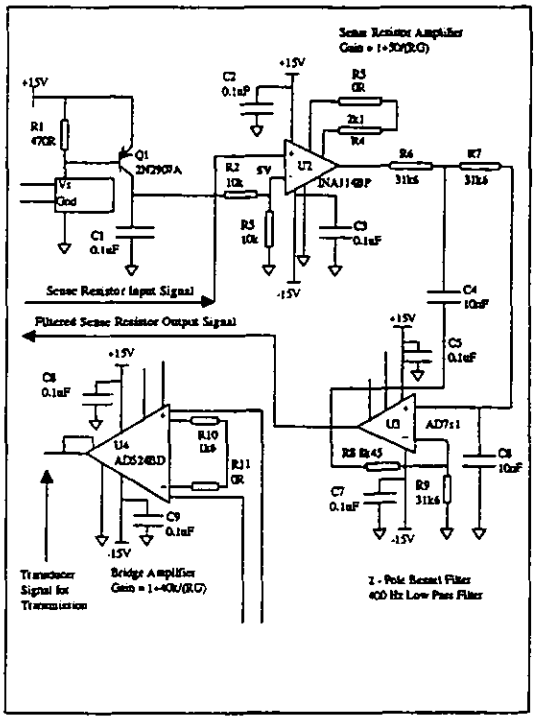

Fig. 7. Pressure Transducer Signal Conditioning Circuitry.

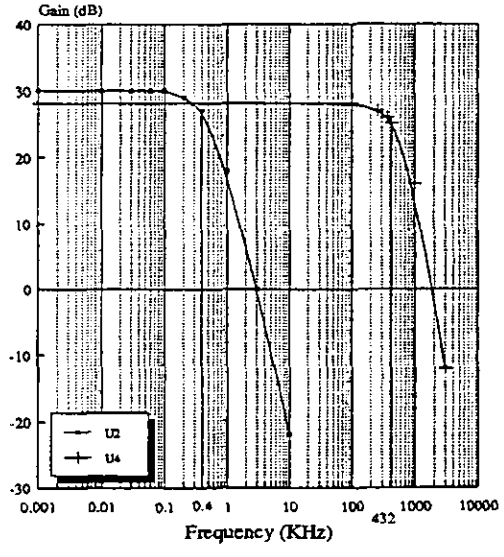

Fig. 8. Filtered pressure transducer sense amplifier, U2, and unfiltered bridge amplifier, U4, frequency response curves.

Specification

- 16 channels required for data transmission split between two boards, each board containing 8 channels.
- Each channel of the in shaft system will consist of a voltage-to-frequency converter, designed to produce a 500KHz-1MHz output for a 0-5V amplified input signal, which is connected to infra-red optical diodes.
- The stationary elements of the transmission system will consist of a phase locked loop receiver and output filter.
- The transmission system will be designed to have a bandwidth of 100KHz
- The in-shaft transmission boards will supply power to the heat transfer/pressure transducer boards.

Opto-Electronic System Design

The use of optical diodes requires that the signals to be transmitted must be converted from analog to digital form and this is performed using a Voltage-to-Frequency Converter (V/F). In voltage to frequency conversion, an analog input signal is converted to an output pulse train whose frequency is proportional to the input level. The V/F used is an AD650 and it provides a combination of high frequency operation and low non-linearity. At 1 MHz full scale, nonlinearity is guaranteed to less than 1000ppm (0.1%), which corresponds to 14-bit linearity of an ADC. A block diagram of the data transmission system is shown in Fig. 9.

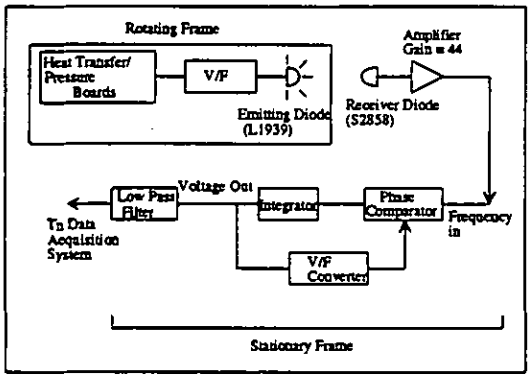

Fig. 9. Single Channel Transmission System Block Diagram.

The system is divided into stationary and rotating components. Components in the rotating frame include a V/F transforming the analog signal into a frequency between 500 KHz and 1MHz and a buffer circuit to drive the emitting diodes. A 500 KHz output signal from the V/F corresponds to zero signal strength. The emitting diodes used are the Hamamatsu L1939 LED's. They are characterised by a very large emission angle and a frequency band of 1 MHz. At 90° from it's principle emission direction, the diode transmits 75% of it's maximum power. Due to the circumference of the shaft that the diodes are to mounted on, five diodes per channel are required to ensure continuous transmission of signals from the rotating to the stationary frame. In the stationary frame, components include a receiver diode with a built in preamplifier, a Frequency-to-Voltage (F/V) converter integrated in a Phase Locked Loop (PLL) circuit, and a low pass filter to filter the residual frequencies of the PLL. The receiver diode, a Hamamatsu S2858 photodiode, is a high speed analog output, high impedance amplifier chip. The distance between the emitter and the receiver diodes has been set at 20mm, but the photodiode can be placed at a distance of up 50mm. This distance was set by mounting 5 diodes, at 72° apart, on a test shaft. The photodiode and amplifier circuit was placed directly opposite this shaft, between two of the diodes. The distance between the emitter and receiver diodes was varied until the optimum output signal was achieved. The Schmitt trigger upper and lower threshold levels were set based on this optimum output signal level.

The receiver diode picks up the emitter signal and produces an electrical reproduction of the transmitted pulse train. The amplitude of this signal is of the order mV and therefore needs to be amplified. This is performed by an AC coupled amplifier with a gain of 40. This signal needs to be converted to a 5V square wave pulse train before being fed to the PLL as the phase detector part of the PLL is composed of digital electronics. A Schmitt trigger recovers the signal and produces this train of pulses which are fed to the PLL section. An active 8 pole 100 KHz butterworth low pass filter was designed to filter out the residual frequencies of the PLL. Initially, a passive filter was used which consisted of inductors, capacitors and resistors, but the design was changed to incorporate the active filter thereby eliminating the inductors which are bulky. Four voltage-controlled voltage-source filter sections are used to construct this 8-pole filter and the gain of each section is set at 1.038, 1.337, 1.889 and 2.610 respectively. Because each of the V/F converters on the transmission boards exhibit slightly different offset frequencies, a procedure has been developed which allows accurate calibration between each channel on the transmission and receiver electronics to maintain linearity error for the complete system to less than 1%. This procedure will be carried out when the boards are installed into the rotor hub and all adjustments will be carried out on the PLL board.

A sine wave of varying frequency and fixed amplitude was applied to the transmission circuits to evaluate both the frequency response and the time delay of the system. The time delay of the system varies from 8μS to 13μS over the entire frequency range and can be seen in Fig. 10. The transmission system frequency response for one channel is shown in Fig. 11 and shows a bandwidth of approximately 78 KHz, which is typical of all other channels. A d.c linearity test was performed on all 16 transmission channels and the response to this test is presented in Fig. 12 for three typical channels. The deviation of the output voltage from the input voltage is less than +/-0.5% over the measured voltage range. Measurement of noise from the transmission system i .e from V/F to the output of the PLL loop, alone indicated values of 1.9120mV RMS, a signal to noise ratio of 68dB, and with a thin film gauge connected to the heat transfer boards transmitted through the transmission system, a value of 7.9mV RMS was recorded.

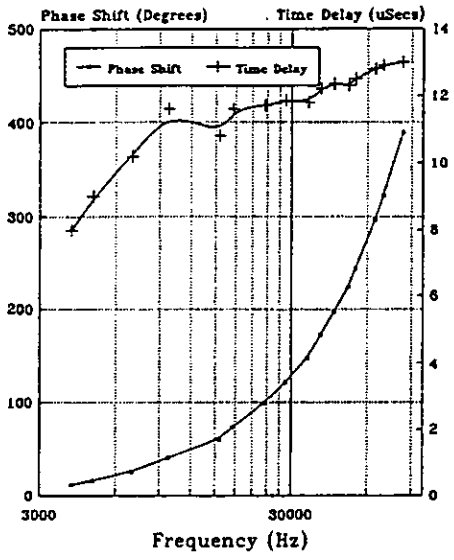

Fig. 10. Delay and Phase shift of the Transmission System.

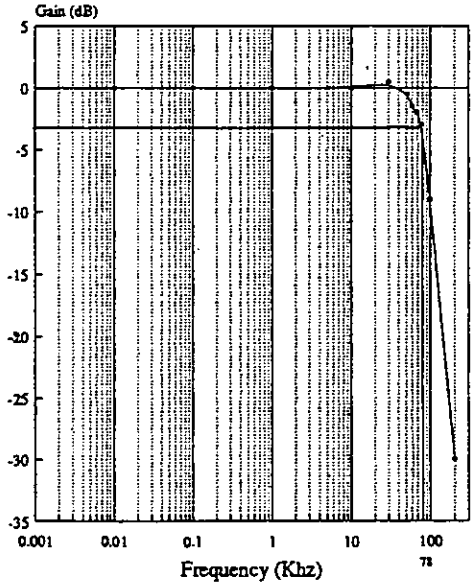

Fig. 11. Typical Transmission system frequency response.

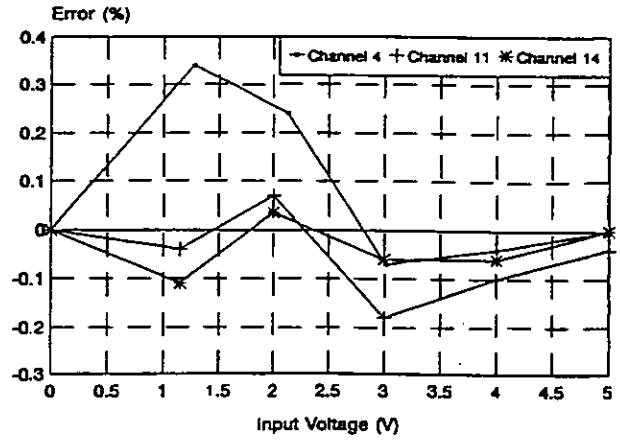

Fig. 12. Error in signal transmission for DC input signals.

MECHANICAL DESIGN, LAYOUT AND STRESS SCREENING

Figure 13 gives details of the layout of the signal conditioning circuitry when it will be placed into the rotor hub. The hub area is large enough to accommodate 4 boards, 2 heat transfer or 2 pressure transducer boards and 2 transmission boards, of equal dimensions, 250mm by 62mm.

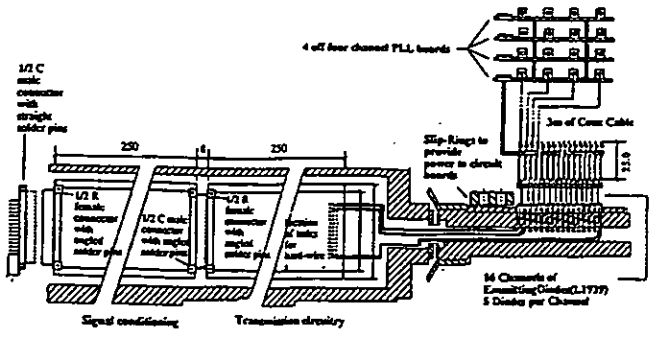

Fig. 13. Section through the hub area showing board and emitter diode connections and receiver board connections to PLL boards.

The two transmission boards will be positioned permanently into the hub where they will be hardwired to each row of LED's, and power supply from the slip-rings. Each of the transmission boards contain eight channels, giving a total of 16 channels and these boards will supply power to the pressure transducer or heat transfer boards. These boards will connect directly into the transmission boards by means of a 3-way 32 pin connector. The instrumentation on the blades will be attached to the signal conditioning boards via a 32 pin

connector. All boards contain through hole components and when placed into the rotor hub, the component side of each board will face inwards. The frequency compensatinn circuitry discussed previously is located on a separate board which is attached to each heat transfer board. Each frequency compensation board with dimensions 58.5mm by 47mm is composed of surface mount components and contains 6 channels, corresponding to the same number on each heat transfer board. A mounting hole present on each of the heat transfer boards provided the means of attaching each frequency compensation board. All power and signal connections to the compensation boards are hardwired from the respective heat transfer board. Figure 14 illustrates the mounting of the additional boards.

On the stationary side, each channel is divided between two circuit boards. All channels have a small receiver board with dimensions 50mm by 25mm. These boards contain a receiver diode and the amplifier circuit. The signal from these boards is transmitted over 3 metres of coaxial cable to one of four PLL boards, each containing four channels, which has dimensions 197mm by 120mm. The four channels all operate from a common power supply and this board also supplies the power for four small receiver boards. For this set to operate from the same supply, they are all linked together. Figure 15 illustrates how a set of 4 receiver boards are linked together and connected to one PLL board.

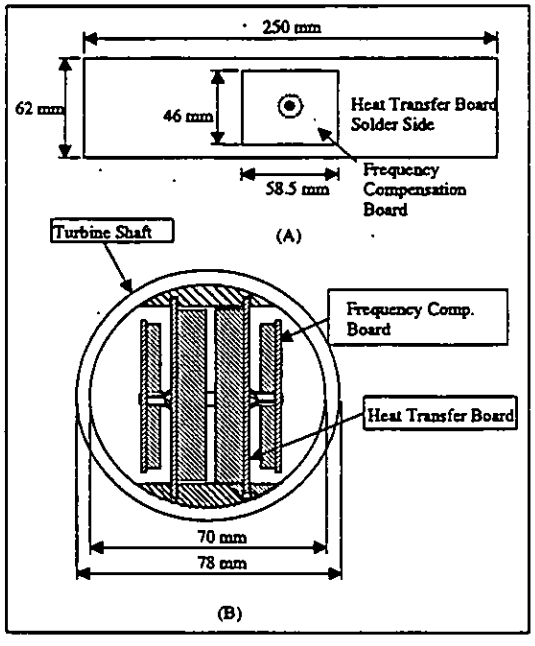

Fig. 14. Frequency Compensation Board mounted on Heat Transfer Board. (A) Side View (B) Axial View.

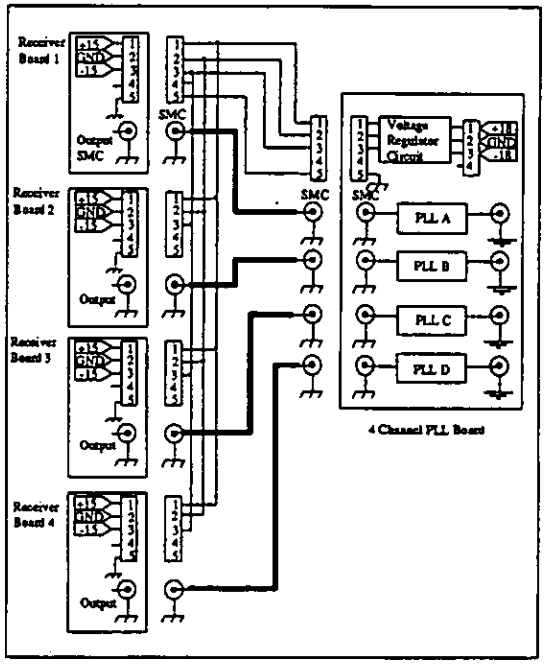

Fig. 15. Four Small Receiver Boards connecting to one PLL Board

To ensure the mechanical integrity of all the boards before being used in the turbine shaft, a stress screening facility was designed and built, Fig. 16. The boards were supported in U-channels, as in the turbine, and the channels were mounted in a steel cylinder between two roller bearings. The cylinder was belt-driven from a lathe which limited the maximum speed to 6,000 rpm. The boards were tested in the stationary mode, then spun to the maximum speed of the rig and tested again. No mechanical problems were detected.

If the system described is installed correctly and properly screened from electrical noise, it should operate in exactly the same way as it had operated under test. The complete heat transfer system has been tested to 2000 rpm with no change in operating parameters.

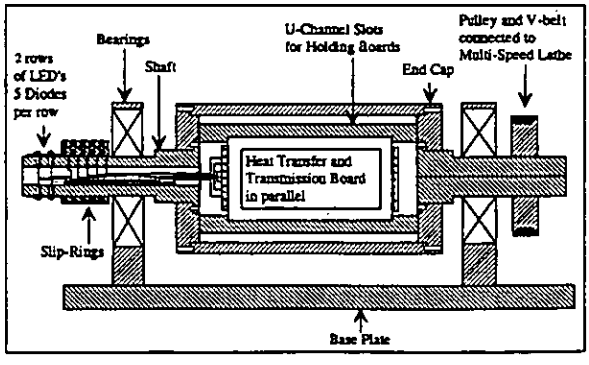

Fig. 16. Side View of Spinning Rig.

.CONCLUSIONS

- Electronic circuits for conditioning heat transfer and pressure data in a transient turbine shaft prior to transmission have been designed and tested.
- A 16 channel optical data transmission system has been developed
- The complete system meets the specification required to resolve blade wake interactions.
- The rotating systems have been successfully mechanically stressed tested to a speed of 6000 rpm.

ACKNOWLEDGEMENTS

The above research is carried out as part of the *BRITE EURAM* Aero 002 Project "Investigation of the Aerodynamics and Cooling of Advanced Engine Turbine Components". The authors wish to acknowledge this financial support and the technical support of Prof. Claus Sieverding of VKI as well as the invaluable contributions by Power Electronics Ireland and Dr. George Gooberman of The University of Limerick.

REFERENCES

Ainsworth, R. W., Allen, J. L., Davies, M. R. D., Doorly, J. E., Forth, C. J. P., 1988a, "Developments in Instrumentation and Processing for Transient Measurement in Full Stage Model Turbine", ASME 33rd International Gas Turbine Conference, Amsterdam, Paper No. 88-GT-11

Ainsworth, R. W., Dietz, A. J., Nunn, T. A., 1991, "The use of Semi-Conductor Sensors for Blade Surface Pressure Measurement in Model Turbine Stage", ASME Journal of Engineering for Gas Turbines and Power, Vol. 113, pp261-268.

Ainsworth, R. W., Shultz, D.L., Davies, M. R. D., Forth, C. J. P., Hilditch, M. A., Oldfield, M. L. G. and Sheard, A. G., 1988b, "A Transient Flow Facility for the Study of the Thermofluid-Dynamics of a full Stage Turbine under Engine Representative Conditions", 33rd ASME International Gas Turbine Conference, Amsterdam, Paper No. 88-GT-144

Davies, M. R. D., Wallace, J. D., 1995 "Gas Turbine Model Scaling", Presented at the International Gas Turbine and Aeroengines Congress and Exposition, Houston, Texas, June 5-8, Paper No. 95-GT-205.

Denton, J. D., 1993, "Loss Mechanisms in Turbomachines", Journal of Turbomachinery, pp 621-656, Vol. 115, October.

Doorly, D. J., Oldfield, M. L. G., 1985a, "Simulation of Wake Passing in a Stationary Turbine Rotor Cascade", Journal of Propulsion, pp 316-318, Vol. 1 No. 4, July.

Doorly, D. J., Oldfield, M. L. G., 1985b, "Simulation of the Effects of Shock Wave Passing on a Turbine Rotor Blade", ASME Paper No. 85-GT-112.

Doorly, D. J., Oldfield, M. L. G., Scrivener, C. T. J., 1989, "Wake passing in a turbine rotor cascade", Agard CP-390, Bergen, Norway.

Dring, R. P., 1982, "Turbine Rotor-Stator Interaction", ASME Paper No. 82-GT-3.

Dunn, M. G., George, W.K., Rae, W. J., Woodward, S. H., Moeller, J. C., Seymour, P.J., 1986, "Heat Flux Measurements for the Rotor of a full Stage Turbine : Part II - Description of Analysis Technique and Typical Time Resolved Measurements", Journal of Turbomachinery, pp. 287-293, Vol. 108.

Dunn, M. G., Lukis, G., Urso, M., Hiemenz, R. J., Orszulak, R. L., Kay, N. J., 1984, "Instrumentation for Gas Turbine Research in Short-Duration Facilities", Aerospace Congress, Long Beach, CA, Paper No. 841504, 15th-18th October.

Dunn, M. G., Seymour, P.J., Woodward, S. H., George, W.K., Chupp, R. E., 1989, "Phase-Resolved Heat Flux Measurements on the Blade of a Full-Scale Rotating Turbine", Journal of Turbomachinery, pp. 8-19, Vol. 111, January1989.

Dunker, R., 1995, "Advances in Engine Technolgy", Wiley

Hodson, H. P., 1983, "Boundary Layer and Loss Measurements on the Rotor of an Axial Flow turbine", ASME Paper No.83-GT-4.

Johnson, A.B., Oldfield, M. J. G., Ainsworth, R. W., Oliver, M. J., 1989, "Surface Heat Transfer Fluctuations on a Turbine Rotor Blade due to upstream Shock Wave Passing", Journal of Turbomachinery, pp105-115, Vol. 111, April 1989.

Kappler, G., Wolfgang, E., Horst, B., 1987, "Rotating Opto-Electronics Data Transmitter for Local Heat Transfer Measurements", ICI-ASF'87 record, pp 77-82.

Oldfield, M. L. G., Jones, T. V., Schultz, D. L., 1978, "On-line Computer for Transient Turbine Cascade Instrumentation", I.E.E.E. Transactions on Aerospace and Electronic Systems, Vol. AES-14, No. 5, pp 738-749.

Sieverding, C. H., Arts, T., 1992 "The VKI Compression Tube Annular Cascade Facility CT3", Presented at the International Gas Turbine and Aeroengine Congress and Exposition, Cologne, Germany, June 1-4.

Sieverding, C. H., Vanhaeverbeek, C., Schulze, G., 1992, "An Opto-Electronic Transmission System for Measurements on Rotating Turbomachinery Components", Paper 92-GT-337, International Gas Turbine and Aeroengine Congress and Exposition, Cologne, Germany, June 1-4.